Materials Physics and Mechanics 36 (2018) 1-7 Received: January 10, 2018

COMPOSITION AND CONTACT ANGLE OF Au-III-V DROPLETS ON TOP OF Au-CATALYZED III-V NANOWIRES

V.G. Dubrovskii*, Zh.V. Sokolova, M.V. Rylkova, A.A. Zhiglinsky

ITMO University, Kronverkskiy pr. 49, St. Petersburg, 197101, Russia

*e-mail: dubrovskii@mail.ioffe.ru

Abstract. We present a model which allows for the self-consistent determination of the stationary group III and V concentrations in the droplet and the contact angle versus the group III and V fluxes during the Au-catalyzed vapor-liquid-solid growth of III-V nanowires. The nanowire axial growth rate in the mononuclear regime is taken in the Zeldovich form. Chemical potentials of the group III and V atoms in liquid are considered within the regular solution model. We show how the group III content and the droplet contact angle can be increased be either decreasing group V flux or increasing group III flux. The group V concentration usually decreases for higher contact angles. Overall, these results can be used for modeling and fine tuning of the droplet shapes and compositions influencing the morphology and the preferred crystal structure of Au-catalyzed III-V nanowires in different epitaxy techniques.

Keywords: III-V nanowires; droplet composition; contact angle; VLS growth.

1. Introduction

Semiconductor nanowires (NWs) and in particular III-V NWs grown by the vapor-liquid-solid (VLS) method are widely considered as promising building blocks for fundamental nanoscience and nanotechnology [1, 2]. It has been known for a long time that the contact angle of an Au-III-V alloy catalyzing the VLS growth of III-V NW may affect its growth rate and morphology [3]. More recently, it has been found that the preferred crystal structure of most III-V NWs can be tuned by the growth conditions between the zinc blende (ZB) and wurtzite (WZ) phase, and is largely influenced by the droplet composition and contact angle [4-6]. Furthermore, *in situ* growth monitoring reveals the possibility of forming truncated growth interface. Truncation is absent at smaller contact angles and present at larger contact angles [7, 8]. III-V NWs catalyzed by smaller contact angle droplets usually show planar growth interface and the WZ structure, changing to truncated interface and the ZB structure when the contact angle is increased above a certain threshold [8]. The droplet composition is also important for understanding and controlling the VLS growth of ternary III-V NWs and their axial heterostructures in connection with the droplet stability issue [9, 10].

Due to a high volatility of the arsenic and phosphorous growth species, the droplet composition is actually determined by the III/V ratio. The composition can be tuned simply by changing the atomic fluxes of the group V and III elements, as in Refs. [8, 9]. It is intuitively clear that higher V/III flux ratios should yield smaller droplets and lower group III concentrations, while lower V/III ratios should lead to a droplet swelling due to its higher group III content. However, quantitative description of the droplet shape and composition versus fluxes seems to be lacking in the literature. Consequently, here we present a self-consistent model, which describes the droplet composition in Au-catalyzed III-V NWs,

http://dx.doi.org/10.18720/MPM.3612018_1

including the group V concentration, in the most common case of mononuclear nucleation-limited VLS growth [5].

2. Model

We define the atomic concentrations of different atoms in a ternary Au-III-V droplet according to $c_i = N_i/(N_3 + N_5 + N_{Au})$ for i = group III (3), group V (5) and Au, with N_i as the number of atoms of type i dissolved in the droplet. We will use the condition $c_5 << 1$ in what follows. Then the droplet volume depends only on the sum of the group III and gold atoms so that $N_3 + N_{Au} = \pi R^3 f(\beta)/(3\Omega_L)$, with Ω_L as the elementary volume in liquid and $f(\beta) = (1-\cos\beta)(2+\cos\beta)/[(1+\cos\beta)\sin\beta]$ as the geometrical function relating the volume of spherical cap to the cube of its base R through the contact angle β. Assuming a constant NW radius $R = const$, the group III concentration and the contact angle are related as

$$c_3 = 1 - \frac{f(\beta_0)}{f(\beta)}(1 - c_3^0). \quad (1)$$

Therefore, finding c_3 as a function of β requires only one measurement of the group III concentration and the corresponding contact angle, say, c_0 and β_0, as in Ref. [10]. This relationship is shown in Fig. 1 assuming c_0=0 at β_0=90°.

Kinetic equations governing the time evolution of N_3 and N_5 are given by [11, 12]

$$\frac{dN_3}{dt} = \frac{\pi R^2}{\Omega_S}[\chi_3 v_3 - G(\Delta\mu)],$$
$$\frac{dN_5}{dt} = \frac{\pi R^2}{\Omega_S}\left[\chi_5 v_5 - \frac{2}{(1+\cos\beta)} v_5^0 e^{2\mu_5} - G(\Delta\mu)\right]. \quad (2)$$

Here, v_i are the atomic fluxes for $i = 3$ and 5, χ_i summarize the geometrical growth effects, and Ω_S is the elementary volume per III-V pair in solid (0.0452 nm^3 for GaAs). The desorption rate for the group V atoms is taken proportional to $\exp(2\mu_5)$ for As_2 or P_2 vapor, as in Refs. [12, 13], with μ_5 as chemical potential of the group V atoms in liquid and v_5^0 as the temperature-dependent desorption constant. The axial NW growth rate G is a function of the liquid-solid chemical potential difference per III-V pair, $\Delta\mu = \mu_3 + \mu_5 - \mu_{35}^0$, with μ_3 as chemical potential of the group III atoms in liquid and μ_{35}^0 as the reference value of chemical potential for a III-V pair in solid [14]. In the first equation, we take into account the arrival rate of the group III atoms and their sink due to the NW growth, while the second equation additionally describes the group V desorption. The sink $-G(\Delta\mu)$ should be identical for both types of atoms to ensure that solid is stoichiometric, and actually regardless of the particular form of the $\Delta G(\Delta\mu)$ dependence.

According to the current view [2, 5, 6, 12, 13], the VLS growth of NWs in mononuclear, yielding the $G(\Delta\mu)$ dependence of the form

$$G(\Delta\mu) = \pi R^2 h J(\Delta\mu) \cong \pi R^2 h J_* \exp\left(-\frac{A}{\Delta\mu}\right), \quad (3)$$

with h as the height of III-V monolayer (0.326 nm for <111>-oriented GaAs NWs). The simplified expression in the right hand side neglects weak pre-exponential factors with respect to the extremely steep exponential term in the Zeldovich nucleation rate $J(\Delta\mu)$, as usual in

nucleation theory [15, 16]. In the particular case of Au-catalyzed III-V NWs, this result follows from Ref. [17]. The J_* factor in Eq. (3) summarizes these almost constant terms.

The A constant under the Zeldovich exponent is given by [17]

$$A = 3^{3/2}(\gamma_{eff}/k_BT)^2\Omega_S h, \tag{4}$$

with γ_{eff} as the effective surface (or edge) energy of regular triangle island, T as the growth temperature and k_B as the Boltzmann constant. For all VLS systems, the A value must be much larger than unity – otherwise, the islands cannot be stable against thermal fluctuations.

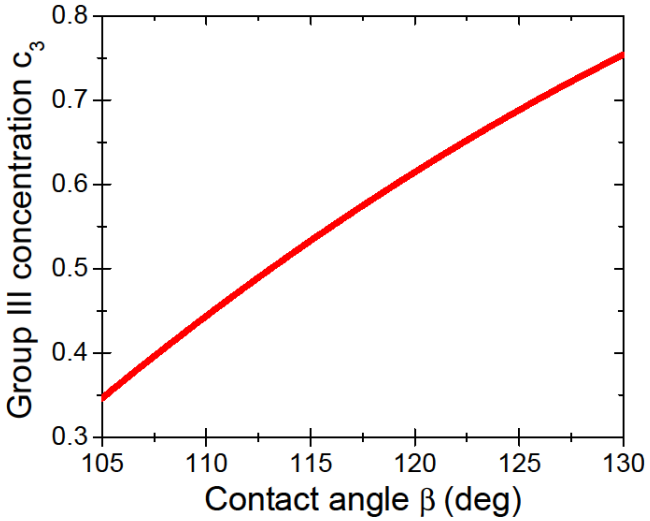

Fig. 1. Group III concentration versus the droplet contact angle for c_0=0 at β_0=90°.

Chemical potentials in liquid can be described within the regular solution model [14]

$$\mu_3 = \mu_3^0 + \ln c_3 + \omega_{35}c_5^2 + \omega_{3Au}(1-c_3-c_5)^2 + (\omega_{35}+\omega_{3Au}-\omega_{5Au})c_5(1-c_3-c_5)+\ldots \cong \mu_3^0 + \ln c_3 + \omega_{3Au}(1-c_3)^2, \tag{5}$$

$$\mu_5 \cong \mu_5^0 + \ln c_5 + \omega_{35}c_3^2 + \omega_{5Au}(1-c_3-c_5)^2 + (\omega_{35}+\omega_{5Au}-\omega_{3Au})c_3(1-c_3-c_5)+\ldots \cong \mu_5^0 + \ln c_5 + \omega_{35}c_3^2 + \omega_{5Au}(1-c_3)^2 + (\omega_{35}+\omega_{5Au}-\omega_{3Au})c_3(1-c_3). \tag{6}$$

Here, μ_i^0 are chemical potentials of pure liquids and ω_{ik} are the binary interaction constants of *i* and *k* atoms in liquid, in thermal units of k_BT. The approximate expressions in the right hand sides corresponds to the approximation $c_5 \to 0$, which does not much change the chemical potential values due to the smallness of c_5. Very importantly, in this approximation μ_3 becomes independent of c_5 as noticed earlier Ref. [13], while μ_5 contains only the material-independent logarithmic dependence on c_5.

The stationary ($dN_3/dt = 0$) solution to Eq. (2) for the group III atoms yields $G(\Delta\mu) = \chi_3 v_3$. Using this in Eq. (2), chemical potential of the group V atoms in the droplet is obtained as [13]

$$\mu_5 = (1/2)\ln\left[\frac{(1+\cos\beta)}{2v_5^0}(\chi_5 v_5 - \chi_3 v_3)\right]. \tag{7}$$

Using this μ_5 in the approximate Eq. (6), we get the group V concentration in the form

$$c_5 = \frac{1}{Y(c_3)}\left[\frac{(1+\cos\beta)}{2k_5^{des}}(\chi_5 v_5 - \chi_3 v_3)\right]^{1/2} \quad (8)$$

with

$$Y(c_3) = \exp[\omega_{35}c_3^2 + \omega_{5Au}(1-c_3)^2 + (\omega_{35} + \omega_{5Au} - \omega_{3Au})c_3(1-c_3)] \quad (9)$$

and $k_5^{des} = v_5^0 \exp(2\mu_5^0)$. On the other hand, using Eq. (7) in the stationary Eq. (2) for the group III atoms along with the approximate Eq. (3) yields

$$\chi_5 v_5 - \chi_3 v_3 = k_5^{des} \exp\left\{\frac{2A}{\ln[\pi R^2 h J_*(1+\cos\beta)/(2v_3)]} - 2F(c_3)\right\} \quad (10)$$

with

$$F(c_3) = \Delta\mu_{35}^0 + \ln c_3 + \omega_{3Au}(1-c_3)^2, \quad (11)$$

and $\Delta\mu_{35}^0$ as the liquid-solid chemical potential difference for pure materials.

Considering that A, k_5^{des}, J_*, $\Delta\mu_{35}^0$ and ω_{ik} are known, Eqs. (8) to (11) give explicitly the stationary compositions c_3 and c_5 versus fluxes. Indeed, the contact angle is related to c_3 according to Eq. (2) and the χ_i are the known functions of β. In metal organic vapor phase epitaxy (MOVPE) or hydride vapor phase epitaxy (HVPE), we have simply $\chi_3 = \chi_5 = 2/(1+\cos\beta)$. In molecular beam epitaxy (MBE), the χ_i are given by the expressions of Ref. [18] and depend on the flux incident angles, with the simplest case being $\chi_3 = \chi_5 = 1/\sin^2\beta$ (this requires large enough droplets). The diffusion-induced radius-dependent contributions [19] for the group III adatoms may also be taken into account in χ_3. Hence, the c_3 versus fluxes is obtained from Eqs. (10) and (11), which are independent of c_5. Using the obtained c_3 versus fluxes in Eqs. (8) and (9), we in turn get explicitly c_5 versus fluxes.

3. Results and discussion

As a general observation, the v_3 and v_5 fluxes enter differently the stationary Eq. (10), which is why the stationary droplet composition (as well as its non-stationary variation at after the flux tuning) is not a function of the V/III flux ratio v_5/v_3 or the V/III flux imbalance $\chi_5 v_5 - \chi_3 v_3$. Another observation is that the $F(c_3)$ in Eq. (11) increases with increasing c_3 when $\omega_{3Au} < 0$, which is why lower $\chi_5 v_5 - \chi_3 v_3$ in Eq. (10) require larger c_3, corresponding to larger droplets. This explains the droplet swelling with decreasing the V/III influx imbalance. Very importantly, Eq. (8) shows that VLS III-V NWs cannot grow at all, when $\chi_5 v_5 - \chi_3 v_3$ is negative, because of the group V desorption, which is always present. The stationary group V concentration decreases for lower $\chi_5 v_5 - \chi_3 v_3$, that is, we should normally expect lower group V atoms in larger droplets (which might seem counter-intuitive at first glance).

We have performed calculations in the MOVPE (or HVPE) case $[\chi_3 = \chi_5 = 2/(1+\cos\beta)]$ without surface diffusion of the group III adatoms, for GaAs NWs at 500 ^{o}C. Other parameters are listed I Table 1. The composition-independent binary interaction constants ω_{ik} and the $\Delta\mu_{GaAs}^0$ value are based on the data of Ref. [20]. It is seen that even a relatively low value of γ_{eff} of 0.25 J/m^2 yields a large A of 41.6. This justifies the approximation made in Eq. (3), that is, leaving only the leading exponential dependence of

the Zeldovich nucleation rate on $\Delta\mu$. Figure 2 shows the expected increase of the droplet contact angle with decreasing $v_5 - v_3$. It is interesting to note that the droplet shape is less sensitive to the V/III flux imbalance at high $v_5 - v_3$, while the droplet swelling becomes very fast as the imbalance approaches zero. In the absence of surface diffusion, smaller NW radii yield larger contact angles and consequently Ga contents. Increasing v_3 at a fixed $v_5 - v_3$ leads to a very significant increase of the contact angle, showing that the droplet shape and composition is not determined by the sole parameter $v_5 - v_3$, but also depend on the absolute value of v_3.

Table 1. Parameters used in calculations for GaAs NWs at 500 ^{o}C.

ω_{GaAs}	ω_{GaAu}	ω_{AsAu}	$\Delta\mu^{0}_{GaAs}$	γ_{eff}, J/m^2	A	k^{des}_{As}, nm/s	J_*, 1/nm^{2}s
-4.488	-9.517	1.101	11.80	0.196	41.6	30 000	10 000

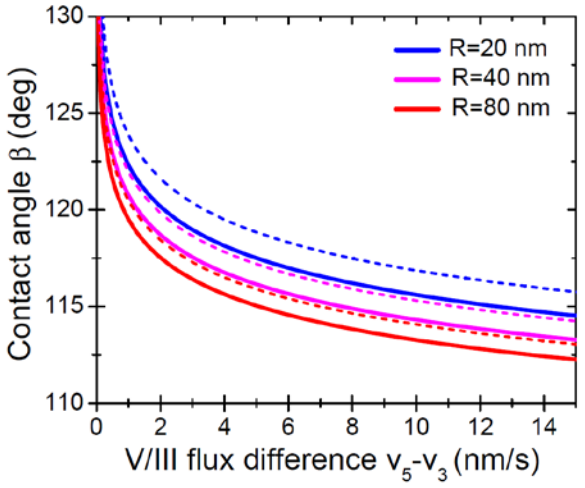

Fig. 2. Contact angle of the Au-Ga-As droplet versus the V/III flux difference $v_5 - v_3$ at R = 20, 40, and 80 nm. The solid and dashed lines correspond to v_3 = 0.5 nm/s and 1.5 nm/s, respectively.

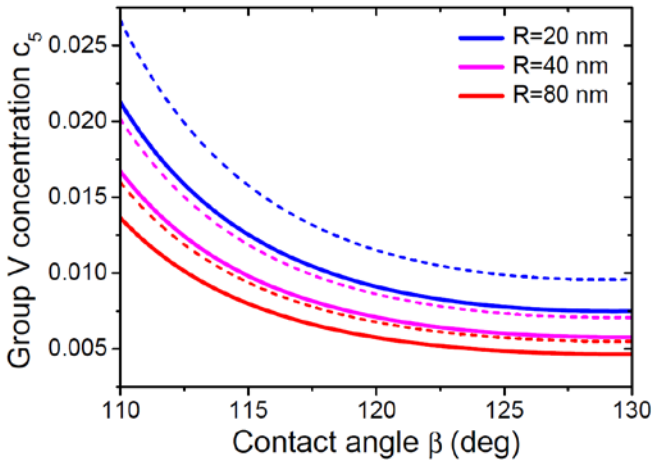

Fig. 3. Arsenic concentration versus the droplet contact angle at R = 20, 40, and 80 nm. The solid and dashed lines correspond to v_3 = 0.5 nm/s and 1.5 nm/s, respectively.

Figure 3 shows the As concentration versus the droplet contact angle for the same parameters as in Fig. 2.

The As content decreases with increasing the contact angle or, equivalently, the gallium content in the droplet. This can be very important for understanding the oscillatory behavior of truncated growth interface in III-V NWs [7, 8] in connection with the so-called stopping effect which becomes more probable for lower As concentrations [21]. The droplets have less As atoms for larger radii NWs, as found previously in the case of Ga-catalyzed VLS growth [12]. This effect is due to the presence of the πR^2 factor in the mononuclear axial growth rate, requiring lower arsenic concentrations for the same G. Higher group III fluxes yield larger c_5 for the same contact angle. This again might seem counter-intuitive. However, depositing more Ga requires that its consumption is also faster, corresponding to higher As concentration for the same Ga content in the droplet to increase the chemical potential.

In conclusion, our model is capable of quantitatively describing the droplet composition and contact angle versus the material fluxes in the VLS growth of Au-catalyzed III-V NWs under the stationary conditions. Our discussion was phrased in terms of MOVPE or HVPE growth. Modeling of MBE growth can be performed using the same approach but with different geometrical factors and including surface diffusion of the group III adatoms along the NW sidewalls. The next step will be studying the time-dependent shapes and compositions following the flux tuning. Overall, these results may be useful for understanding and controlling the droplet compositions influencing the morphology and polytypism of VLS III-V NWs grown by different epitaxy techniques.

Acknowledgements*. The authors thank the Ministry of Education and Science of the Russian Federation for financial support under grant 14.587.21.0040 (project ID RFMEFI58717X0040).*

References

[1] A. Zhang, G. Zheng, C. M. Lieber, *Nanowires: building blocks for nanoscience and nanotechnology* (Springer, 2016).

[2] V.G. Dubrovskii, In: *Semiconductors and Semimetals ser., Semiconductor Nanowires I: Growth and Theory*, ed. by A. Fontcuberta i Morral, S.A. Dayeh and C. Jagadish, (Burlington, Academic Press, 2015), Vol. 93, p. 1-78.

[3] V.G. Dubrovskii, I.P. Soshnikov, G.E. Cirlin, A.A. Tonkikh, Yu.B. Samsonenko, N.V. Sibirev, V.M. Ustinov // *Physica Status Solidi B* **241** (2004) R30.

[4] F. Glas, J.C. Harmand, G. Patriarche // *Physical Review Letters* **99** (2007) 146101.

[5] V.G. Dubrovskii, N.V. Sibirev, J.C. Harmand, F. Glas // *Physical Review B* **78** (2008) 235301.

[6] E. Gil, V.G. Dubrovskii, G. Avit, Y. André, C. Leroux, K. Lekhal, J. Grecenkov, A. Trassoudaine, D. Castelluci, G. Monier, R. M. Ramdani, C. Robert-Goumet, L. Bideux, J. C. Harmand, F. Glas // *Nano Letters* **14** (2014) 3938.

[7] C.-Y. Wen, J. Tersoff, K. Hillerich, M.C. Reuter, J.H. Park, S. Kodambaka, E.A. Stach, F. Ross // *Physical Review Letters* **107** (2011) 025503.

[8] D. Jacobsson, F. Panciera, J. Tersoff, M.C. Reuter, S. Lehmann, S. Hofmann, K.A. Dick, F.M. Ross // *Nature* **531** (2016) 317.

[9] D.L. Dheeraj, A.M. Munshi, M. Scheffler, A.T.J. van Helvoort, H. Weman, B.O. Fimland // *Nanotechnology* **24** (2013) 015601.

[10] V. Zannier, D. Ercolani, U.P. Gomes, J. David, M. Gemmi, V.G. Dubrovskii, L. Sorba // *Nano Letters* **16** (2016) 7183.

[11] V. Zannier, F. Rossi, V.G. Dubrovskii, D. Ercolani, S. Battiato, L. Sorba // *Nano Letters* **18** (2018) 167.

[12] F. Glas, M.R. Ramdani, G. Patriarche, J.C. Harmand // *Physical Review B* **88** (2013) 195304.
[13] V.G. Dubrovskii // *Applied Physics Letters* **104** (2014) 053110.
[14] F. Glas // *Journal of Applied Physics* **108** (2010) 073506.
[15] V.G. Dubrovskii // *Physica Status Solidi B* **171** (1992) 345.
[16] V.G. Dubrovskii // *Journal of Chemical Physics* **131** (2009) 164514.
[17] V.G. Dubrovskii, J. Grecenkov // *Crystal Growth and Design* **15** (2015) 340.
[18] F. Glas // *Physica Status Solidi B* **247** (2010) 254.
[19] V.G. Dubrovskii, N.V. Sibirev, R.A. Suris, G.E. Cirlin, J.C. Harmand, V.M. Ustinov // *Surface Science* **601** (2007) 4395.
[20] E.D. Leshchenko, M. Ghasemi, V.G. Dubrovskii, J. Johansson // *CrystEngComm* **20** (2018) 1649.
[21] V.G. Dubrovskii // *Crystal Growth and Design* **17** (2017) 2589.